the magnetic field AA, and whose walls BB are perfectly conducting for $x < 0$ and non-conducting for $x > 0$. Then, when the Hartmann number $M \geqslant 1$, the velocity expressed in terms of the pressure gradient is $O(M^{-2})$ when $x < 0$ and $O(M^{-1})$ when $x > 0$, so that some shear layer must exist near $x = 0$. Although Yakubenko obtained an exact solution to this problem by means of the Wiener–Hopf technique he did not interpret the result physically nor did he produce any numerical data.

Waechter (1966) has recently analysed the flow in the same long duct in which there is no pressure gradient, the walls AA are non-conducting, the wall B at $y = a$, for $x < 0$ is perfectly conducting and held at a potential ϕ_0, the wall B at $y = -a$ for $x < 0$ is also perfectly conducting but held at a potential $-\phi_0$, and both the walls BB are non-conducting for $x > 0$. In this case there is no flow in the core when $x < 0$ and therefore no discontinuity in the velocity. However, there is a discontinuity at $x = 0$ in $\partial\phi/\partial y$, which necessitates the existence of a layer at $x = 0$ in which the velocity is non-zero. Such a layer was first discussed by Moffatt (1964) who examined the case where the wall at $y = a$ is perfectly conducting and held at a potential ϕ_0 for $x > 0$ and for $x < 0$ is also perfectly conducting but held at zero potential. There has to be an infinitely small insulating segment of wall at $x = 0$. The wall at $y = -a$ is perfectly conducting and held at zero potential. Again in this case there is a layer at $x = 0$, through which $\partial\phi/\partial y$ is discontinuous and in which the velocity is non-zero. Moffatt discussed in detail the physics of such a layer, through which there is a discontinuity in the electric field parallel to it, so that we now have a clear physical picture of what to expect when such a discontinuity occurs. However, there were some anomalies in his mathematical solution which Waechter (1966) subsequently clarified.

Alty (1966) examined an altogether more difficult problem; he undertook a theoretical and *experimental* investigation of the pressure driven flow in a square duct, of which two walls are highly conducting and two non-conducting, when a uniform magnetic field is imposed at an arbitrary angle to the walls. By only considering the flow when $M \gg 1$, by dividing the flow up into various regions, which he investigated in turn, and by using some of the results of Moffatt's (1964) analysis he was able to provide an approximate asymptotic analysis in which he discovered the existence of thin layers emanating from the corners of the duct in the direction of the magnetic field. In these layers the velocity and electric field changed discontinuously, in a similar way to the layers of Yakubenko and Moffatt. The existence of these layers was confirmed by the experiments, though indirectly from pressure and electric potential measurements at the walls, no probes being inserted into the flow.

The main interest in these studies has been on the curious layers which emanate in the direction of the magnetic field from the places where the conductivity changes. In each case different layers are found; yet, despite their similarities, a complete analysis and description of these layers in pressure or electrically driven flows is still awaited. The mathematical difficulty is similar to that of analysing MHD duct flows in that *two* coupled linear partial differential equations of second order must be solved (equations (2.4) and (2.5) of Hunt & Stewartson (1965)). These equations may be decoupled by increasing their order

as shown by Braginskii (1960), though in that case the boundary conditions for the various parameters, e.g. velocity and potential, then become coupled, this being the method of Moffatt and Waechter. This method is only suitable for the simplest boundary conditions and types of boundary.

The other approach to solving the coupled equations is to add and subtract them, as originally performed by Shercliff (1953), and later by Hunt & Stewartson (1965). Then, provided the current distribution along the boundary is specified, a solution can be obtained so that the problem becomes the transformation of the current boundary condition to that required, e.g. the specification of the potential, or matching to a finitely conducting electrode, which in general requires the solution of an integral equation, one such being that solved in §2 of Hunt & Stewartson (1965). The great advantage of this method, particularly when $M \gg 1$, is that one is dealing with an elliptic second-order equation whose asymptotic properties are fairly well understood. In this paper we adopt the latter approach (suggested by Professor Shercliff) to examine the flow produced by various electrode configurations.

In §2 we examine the simplest situation in which two line electrodes are placed opposite and parallel to each other in parallel non-conducting planes; an electric current travels between the electrodes and a magnetic field is applied perpendicular to the planes. Assuming that the flow is laminar, uniform and incompressible we find an exact solution for arbitrary values of M and an asymptotic solution when $M \gg 1$. We show that these are identical when $M \gg 1$, and how the results may be interpreted in physical terms. We then analyse the flow when the electrodes are displaced relative to each other, the magnetic field remaining in the same direction; this flow is somewhat similar to that discussed by Alty (1966). In §3 we analyse the flow produced by *point* electrodes placed in non-conducting planes opposite each other, again using an exact and an asymptotic solution.

These solutions provide striking examples of the kind of layers or 'wakes' which may be produced in a flow by discontinuities in the electrical boundary conditions when a strong magnetic field is applied to the fluid. The attraction of these particular layers is that they can be examined experimentally very much more easily than those produced by bodies moving through fluids and in a later paper it is hoped to publish the results of experiments by Hunt & Malcolm, which convincingly demonstrated the existence of these layers.

2. Two-dimensional electrode configuration

2.1. *The equations*

We consider the steady flow of an incompressible fluid with uniform properties driven by the interaction of imposed electric currents and a uniform, transverse magnetic field. In this section we consider two-dimensional situations, in which all the physical variable, including *pressure*, and the boundary conditions are functions of x and y only. Therefore any external circuit connected to the conducting walls of the duct is continuous and unvarying in the z-direction. (This condition may be relaxed if the magnetic field due to the applied currents is small compared to the imposed magnetic field.) We can apply the same unique-

ness theorem to this situation as was developed by Hunt (1968) for fully developed MHD duct flows the only difference being that the pressure gradient dp/dz is zero. Therefore if we can construct a solution consistent with the boundary conditions it is the correct one. We will assume that there is only one component of velocity (in the z-direction) and since this assumption provides a solution we are justified in making it. Then, using the axes defined in figure 1, the equations describing such flows are the same as those of MHD duct flow (Hunt & Stewartson 1965) but with $dp/dz = 0$,

$$j_x = \sigma(-\partial\phi/\partial x - v_z B_0), \quad j_y = \sigma(-\partial\phi/\partial y), \tag{2.1}$$

$$\frac{\partial j_x}{\partial x} + \frac{\partial j_y}{\partial y} = 0, \tag{2.2}$$

$$j_x = \partial H_z/\partial y, \quad j_y = -\partial H_z/\partial x, \tag{2.3}$$

$$0 = -\frac{\partial}{\partial x}(p + H_z^2/2\mu) = -\frac{\partial}{\partial y}(p + H_z^2/2\mu), \tag{2.4}$$

$$0 = j_x B_0 + \tilde{\eta}\left(\frac{\partial^2 v_z}{\partial x^2} + \frac{\partial^2 v_z}{\partial y^2}\right), \tag{2.5}$$

where j_x, j_y, v_z and H_z, are components of current density, velocity and magnetic field, respectively. From (2.3) it follows that H_z may be regarded as a current stream function (i.e. that the lines of constant H_z are parallel to the current). ϕ is the electric potential. B_0, μ, $\tilde{\eta}$ are the flux density of the applied magnetic field, the magnetic permeability and the viscosity of the fluid respectively. We can ignore (2.4) since we do not consider free surfaces and we can rewrite the rest of the equations to give two coupled second-order partial differential equations in v_z and H_z. By normalizing in terms of some reference value of H_z, H_1 say, such that,

$$v = (\sigma\tilde{\eta})^{\frac{1}{2}} v_z/H_1, \quad h = H_z/H_1, \tag{2.6}$$

and $\xi = x/a$, $\eta = y/a$ where a is some characteristic length, the governing equations become:

$$\frac{\partial^2 v}{\partial \xi^2} + \frac{\partial^2 v}{\partial \eta^2} + M\frac{\partial h}{\partial \eta} = 0, \tag{2.7}$$

$$\frac{\partial^2 h}{\partial \xi^2} + \frac{\partial^2 h}{\partial \eta^2} + M\frac{\partial v}{\partial \eta} = 0, \tag{2.8}$$

where $M = B_0 a\,(\sigma/\tilde{\eta})^{\frac{1}{2}}$, is the Hartmann number. We can rewrite these equations in terms of X, $(= v + h)$ and Y, $(= v - h)$, as follows:

$$\frac{\partial^2 X}{\partial \xi^2} + \frac{\partial^2 X}{\partial \eta^2} + M\frac{\partial X}{\partial \eta} = 0, \tag{2.9}$$

$$\frac{\partial^2 Y}{\partial \xi^2} + \frac{\partial^2 Y}{\partial \eta^2} - M\frac{\partial Y}{\partial \eta} = 0. \tag{2.10}$$

2.2. *Aligned line electrodes*

We now analyse the flow between two walls at $y = \pm a$ induced by a current I per unit length in the z-direction entering the fluid at a line electrode (i.e. one of vanishingly small width in the x-direction) at $x = 0$, $y = +a$ and leaving the fluid at $x = 0$, $y = -a$. A magnetic field is imposed in the y-direction. Let $H_1 = \frac{1}{2}I$: then the boundary conditions are:

$$\left.\begin{aligned} &\begin{cases} v_z = 0, & H_z = H_1, & x > 0, & y = \pm a, \\ v = 0, & h = 1, & \xi > 0, & \eta = \pm 1, \end{cases} \\ &\begin{cases} v_z = 0, & H_z = -H_1, & x < 0, & y = \pm a, \\ v = 0, & h = -1, & \xi < 0, & \eta = \pm 1. \end{cases} \end{aligned}\right\} \tag{2.11}$$

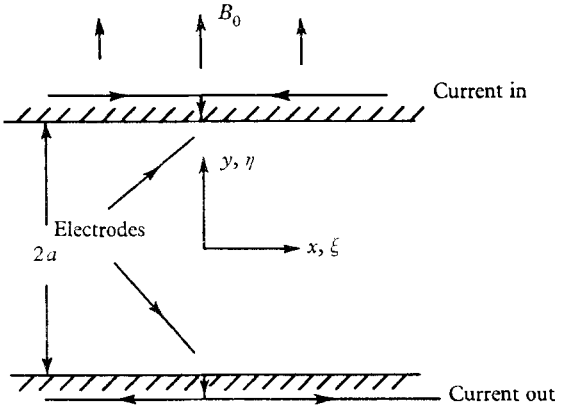

FIGURE 1. Cross-section of the flow induced by line electrodes at $x = 0$, $y = \pm a$ set in insulating planes at $y = \pm a$, with a magnetic field, B_0, in the y-direction.

We can rewrite these boundary conditions in terms of X as

$$\left.\begin{aligned} X &= 1, \quad \xi > 0, \quad \eta = \pm 1, \\ X &= -1, \quad \xi < 0, \quad \eta = \pm 1, \end{aligned}\right\} \tag{2.12}$$

and therefore we need only consider this combined variable. v and H may be found independently from the relations

$$v(\xi, \eta) = \tfrac{1}{2}[X(\xi, \eta) - X(\xi, -\eta)],$$
$$h(\xi, \eta) = \tfrac{1}{2}[X(\xi, \eta) + X(\xi, -\eta)].$$

A solution for X may be obtained by Fourier integral methods. It follows from the identity

$$\int_0^\infty \frac{\sin \alpha \xi}{\alpha} d\alpha = \begin{cases} \frac{1}{2}\pi & (\xi > 0), \\ -\frac{1}{2}\pi & (\xi < 0), \end{cases}$$

that the integral representation

$$X = \frac{2}{\pi} \int_0^\infty g(\eta, \alpha) \frac{\sin \alpha \xi}{\alpha} d\alpha$$

will satisfy the conditions of (2.12) provided that $g(\pm 1, \alpha) = 1$. Equation (2.9) then requires that g has to satisfy

$$\frac{d^2g}{d\eta^2} - \alpha^2 g + M\frac{dg}{d\eta} = 0. \tag{2.13}$$

The solution of (2.13) leads to the final solution for X valid for all values of M namely

$$X = \frac{2}{\pi}\int_0^\infty \left\{\exp\{\tfrac{1}{2}M(1-\eta)\}\frac{\sinh[(1+\eta)\mu]}{\sinh[2\mu]} + \exp\{-\tfrac{1}{2}M(1+\eta)\}\frac{\sinh[(1-\eta)\mu]}{\sinh 2\mu}\right\}\frac{\sin\alpha\xi}{\alpha}\,d\alpha,$$

where

$$\mu = (\tfrac{1}{4}M^2 + \alpha^2)^{\frac{1}{2}}. \tag{2.14}$$

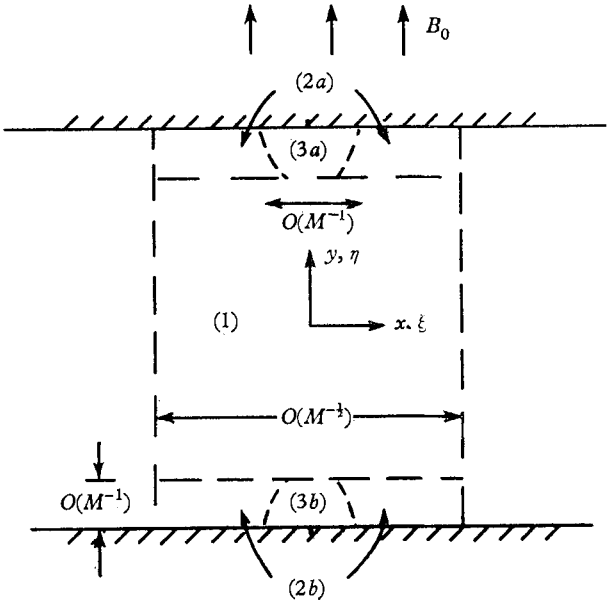

FIGURE 2. Cross-section of the flow showing the regions between the electrodes analysed in the asymptotic analysis of § 2.2 when $M \gg 1$.

Asymptotic solution for large M

As $M \to \infty$ the flow may be examined separately in certain regions. In each of these regions various plausible approximations are made and a complete solution constructed, using standard matching procedures, which is consistent with the approximations and the boundary conditions. In this case the asymptotic solution may also be justified by showing that it is equal to the exact solution as $M \to \infty$. The advantage of our method of asymptotic analysis is that it demonstrates the physical phenomena involved as well as being a method which can be applied to situations where an exact solution is not possible.

Regions (2a) and (2b)

If the thicknesses of the regions (1) and (2) are δ_1 and δ_2, respectively, where $\delta_1 \gg \delta_2$, then in regions (2*a*) and (2*b*)

$$\partial/\partial\eta = O(\delta_2^{-1}) \quad \text{and} \quad \partial/\partial\xi = O(\delta_1^{-1})$$

and $\partial/\partial\eta \gg \partial/\partial\xi$. Therefore (2.9) becomes

$$\frac{\partial^2 X}{\partial \eta^2} + M\frac{\partial X}{\partial \eta} = 0. \tag{2.15}$$

In regions (2*a*) and (2*b*) we are looking for 'boundary layer' solutions to (2.15), so that the requisite boundary conditions for (2*a*) are:

$$\begin{aligned} X &= 1 \quad \text{for} \quad x > 0, \quad \eta = 1, \\ X &= -1 \quad \text{for} \quad x < 0, \quad \eta = 1, \\ X &\to X_1(\eta = 1) \quad \text{as} \quad (1-\eta)M \to \infty, \end{aligned}$$

where $X_1(\eta = 1)$ is the value of the solution for region (1) at $\eta = 1$. The only possible solution for this region then is

$$\begin{aligned} X_{2a} &= \quad 1 \quad \text{for} \quad x > 0, \\ &= -1 \quad \text{for} \quad x < 0, \end{aligned} \tag{2.16}$$

with $X_1 = 1$ for $x > 0$ and $X_1 = -1$ for $x < 0$. The boundary conditions for (2*b*) are:

$$\begin{aligned} X_{2b} &= 1 \quad \text{for} \quad x > 0, \quad \eta = 1, \\ X_{2b} &= -1 \quad \text{for} \quad x < 0, \quad \eta = -1, \\ X_{2b} &\to X_1(\eta = -1) \quad \text{as} \quad (1+\eta)M \to \infty. \end{aligned}$$

To find the solution to this region, we first have to examine region (1).

Region (1)

Since the thicknesses of regions (2*a*) and (2*b*) are small, in region (1) we can assume $\partial/\partial\eta = O(1)$. Since the thickness of region (1) is δ_1, $\partial/\partial\xi = O(\delta_1^{-1})$ and therefore $\partial/\partial\xi \gg \partial/\partial\eta$. The only value of δ_1 which enables us to construct a smooth solution in region (1) satisfying the boundary conditions

$$\begin{aligned} X &= 1, -1 \quad \text{as} \quad x \to \pm\infty, \\ X &= 1, -1 \quad \text{at} \quad \eta = 1 \quad \text{for} \quad x \gtrless 0, \end{aligned}$$

is such that $\partial^2 X/\partial\xi^2$ is of the same order as $M\,\partial X/\partial\eta$. Thus $\delta_1 = O(M^{-\frac{1}{2}})$ and (2.9) becomes:

$$\partial^2 X/\partial\xi^2 + M\,\partial X/\partial\eta = 0. \tag{2.17}$$

The solution to (2.17) is

$$X = \operatorname{erf}\{\sqrt{M}/2(1-\eta)^{\frac{1}{2}}\}. \tag{2.18}$$

We can now write down the value for X in (2b), namely

$$X_{2b} = \exp\{-M(1+\eta)\} + \left[\operatorname{erf}\left(\frac{\xi\sqrt{M}}{\sqrt{8}}\right)\right][1-\exp\{-M(1+\eta)\}] \quad \text{for} \quad x > 0$$

$$= -\exp\{-M(1+\eta)\} + \left[\operatorname{erf}\left(\frac{\xi\sqrt{M}}{\sqrt{8}}\right)\right][1-\exp\{-M(1+\eta)\}] \quad \text{for} \quad x < 0. \tag{2.19}$$

From these solutions we can calculate v and h separately.

In region (1)

$$v = \tfrac{1}{2}\{\operatorname{erf}[\xi\sqrt{M}/2(1-\eta)^{\frac{1}{2}}] - \operatorname{erf}[\xi\sqrt{M}/2(1+\eta)^{\frac{1}{2}}]\}.$$

In region (2a)

$$v = \frac{1}{2}\left\{1-\exp\{-M(1-\eta)\} - \left(\operatorname{erf}\frac{\xi\sqrt{M}}{\sqrt{8}}\right)[1-\exp\{-M(1-\eta)\}]\right\} \quad (x > 0),$$

$$= \frac{1}{2}\left\{-1+\exp\{-M(1-\eta)\} - \left(\operatorname{erf}\frac{\xi\sqrt{M}}{\sqrt{8}}\right)[1-\exp\{-M(1-\eta)\}]\right\} \quad (x < 0).$$

In region (2b)

$$v = \frac{1}{2}\left\{\exp\{-M(1+\eta)\} + \left(\operatorname{erf}\frac{\xi\sqrt{M}}{\sqrt{8}}\right)[1-\exp\{-M(1+\eta)\}] - 1\right\} \quad (x > 0),$$

$$= \frac{1}{2}\left\{-\exp\{-M(1+\eta)\} + \left(\operatorname{erf}\frac{\xi\sqrt{M}}{\sqrt{8}}\right)[1-\exp\{-M(1+\eta)\}] + 1\right\} \quad (x < 0).$$

Similar expressions may be derived for h.†

Regions (3a) *and* (3b)

Both X_{2a} and X_{2b} are discontinuous when $\xi = 0$ and thus there exist regions near the electrodes where no approximations are possible in (2.9). This implies that in these regions all the terms in (2.9) are of the same order and by conventional scaling arguments it follows that these regions, denoted by 3a and 3b, extend a distance $O(M^{-1})$ round the electrodes.

In appendix A we prove that the exact and asymptotic solutions become identical in regions (1) and (2) as $M \to \infty$. The asymptotic form of the exact solution also gives no information as to the regions (3).

The best way to understand the physical reasons for the distribution of velocity and current is to consider what happens to the current and the velocity when the magnetic field is turned on. When there is no magnetic field there is no velocity, and as current passes between the electrodes the current spreads out from the top electrode at least a distance of order a before curving back to the bottom electrode. Let us now consider the quadrant $\xi > 0$, $\eta > 0$ when the magnetic field is applied; the large component of $\mathbf{j} \times \mathbf{B}_0$ accelerates the fluid in the $+z$ direction. However, as v_z *increases*, $v_z B_0$ increases and thus j_x *decreases*. Then, since $j_x B_0$ *decreases*, the acceleration of v_z decreases. This process continues until j_x is reduced to a value sufficient for the $j_x B_0$ force to balance the viscous stresses produced by v_z.

† It is interesting to note that although we can construct a uniformly valid asymptotic solution for X, we cannot do so for v and h separately.

Thus, as we see from figures 3 and 4 in the regions (2*a*) and (2*b*) where the viscous stresses are greatest, i.e. $O(M^2)$, there is a large component of current perpendicular to the magnetic field such that

$$\mathbf{j} \times \mathbf{B}_0 = O(M^2).$$

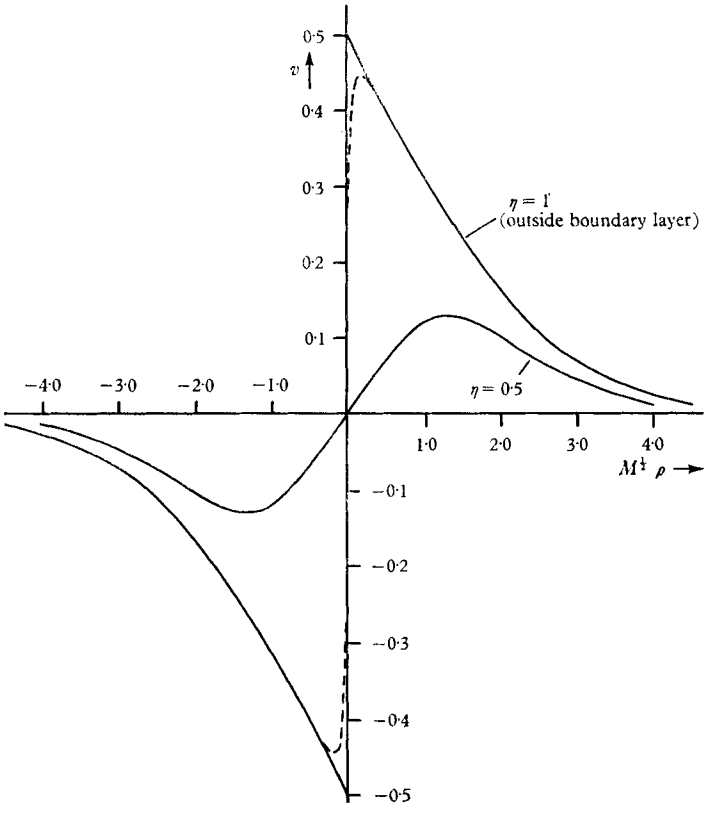

FIGURE 3. Flow between aligned line electrodes; velocity profiles in region (1) at $\eta = 0{\cdot}5$ and $\eta \simeq 1$ (outside the boundary layer). The dotted line indicates how the velocity varies in region (3).

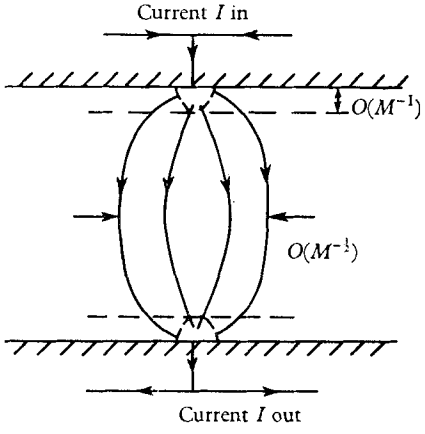

FIGURE 4. Sketch of current streamlines between the aligned line electrodes when $M \gg 1$.

In region (1) however, the viscous stresses are much less, i.e. $O(M)$, and consequently the current has a smaller component perpendicular to B_0.

It is perhaps worth noting that we can construct a solution for electrodes which have a finite thickness, δ where $\delta \ll a$, provided we specify the current distribution on the electrode. Then it is easily shown that as $\delta \to 0$ the solution becomes that of the line electrodes. Therefore our solution is a limit of that solution found by letting the electrode thickness tend to zero.

2.3. *Displaced line electrodes*: (*asymptotic solution*)

We now analyse the flow between two walls when the electrodes are displaced sideways by a distance $2b$ (see figure 5). If $b/a = l$ and $H_1 = \frac{1}{2}I$, the boundary conditions are:

$$\begin{aligned} v = 0, \quad h = X = 1, \qquad & \xi > l, \quad y = a, \\ & \xi > -l, \quad y = -a, \\ v = 0, \quad h = X = -1, \qquad & \xi < l, \quad y = a, \\ & \xi < -l, \quad y = -a. \end{aligned}$$

v and h may be found independently from the relations:

$$\begin{aligned} v &= \tfrac{1}{2}\{X(\xi, \eta) + X(-\xi, -\eta)\}, \\ h &= \tfrac{1}{2}\{X(\xi, \eta) - X(-\xi, -\eta)\}, \end{aligned} \tag{2.20}$$

and it is possible to obtain a Fourier series or Fourier integral solution using a similar method to that in §2.2 (see appendix B). We move straight on to the more interesting asymptotic solution.

We will assume that M is large enough to satisfy the condition that $aM^{-\frac{1}{2}} \ll b$.

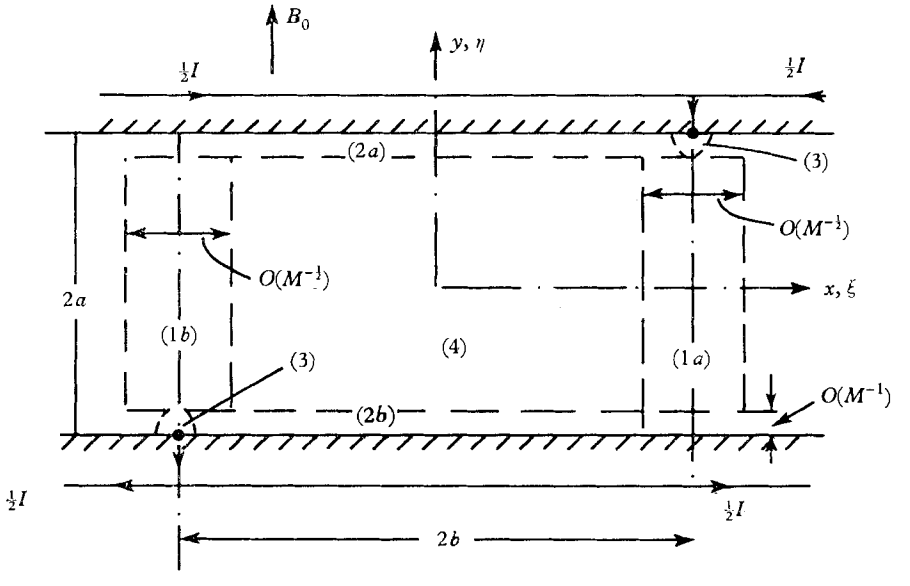

FIGURE 5. Cross-section of the flow induced by displaced line electrodes at $x = b$, $y = a$ and $x = -b$, $y = -a$, showing the regions of the asymptotic analysis.

Then in this situation there is one new type of region not found in the aligned electrode problem. This is the region, (4) (see figure 5), where

$$l-O(M^{-\frac{1}{2}}) > \xi > -l+O(M^{-\frac{1}{2}}),$$
$$1-O(M^{-1}) > \eta > -1+O(M^{-1});$$

in other words this region lies between the Hartmann layers on the walls and the layers of thickness $O(M^{-\frac{1}{2}})$ emanating from the electrodes. In this region both $\partial/\partial\eta$ and $\partial/\partial\xi$ are of $O(1)$ and hence the solution of (2.9) consistent with the boundary conditions is

$$X = -1. \tag{2.21}$$

Therefore

$$v = -1, \quad h = 0. \tag{2.22}$$

The solution for region $(1a)$ is:

$$X = \operatorname{erf}\left[\frac{(\xi-l)\sqrt{M}}{2(1-\eta)^{\frac{1}{2}}}\right], \tag{2.23}$$

and in $(1b)$

$$X = -1.$$

Thus X does not change in $(1b)$ which is to be expected since $X = -1$ in (4) and $X \to -1$ as $\xi \to -\infty$.

The solution for $(2a)$ is much the same as for the aligned line electrode, i.e.

$$X = 1, \qquad \xi > l,$$
$$X = -1, \quad \xi < l,$$

and the solution for $(2b)$ is

$$\xi > -l\text{: } X = -\exp\{-M(1+\eta)\}+\left[\operatorname{erf}\left(\frac{(\xi-l)\sqrt{M}}{\sqrt{8}}\right)\right][1-\exp\{-M(1+\eta)\}];$$

for $(l-\xi)\sqrt{M} \gg 1$, this becomes:

$$X = -1+2\exp\{-M(1+\eta)\},$$

when $\xi < -l$, $X = -1$.

Thus we again must have two regions (3) with thickness $O(M^{-1})$ near the electrodes in which $\partial/\partial\xi$ is of the same order as $\partial/\partial\eta$.

We see from (2.22) that the major difference between this case and the aligned electrode situation is that a net flow is induced. This is simply calculated to be:

$$\int_{-\infty}^{+\infty}\int_{-1}^{+1} v\,d\xi\,d\eta = -4l\left(1-\frac{1}{M}\right),$$

or

$$Q = \int_{-\infty}^{+\infty}\int_{-a}^{+a} v_z\,dx\,dy = -\frac{2Iab}{(\sigma\tilde{\eta})^{\frac{1}{2}}}\left(1-\frac{1}{M}\right). \tag{2.24}$$

The reason for this net flow is that, since the current must pass between the electrodes and since there can be no current in the inviscid core (region (4)), because the flow is steady and there is no pressure gradient, all the current has to pass along Hartmann boundary layers on the two walls, a current $\frac{1}{2}I$ along each. Now Shercliff (1965) has shown that the relation between the total current flowing along a Hartmann boundary layer ($\frac{1}{2}I$ in our case) and the velocity outside it V is

$$V = I/(4\sigma\tilde{\eta})^{\frac{1}{2}},$$

whence we can obtain the first term in our expression for Q. It is important to note that the first term in (2.24) is independent of the value of B_0, though if the

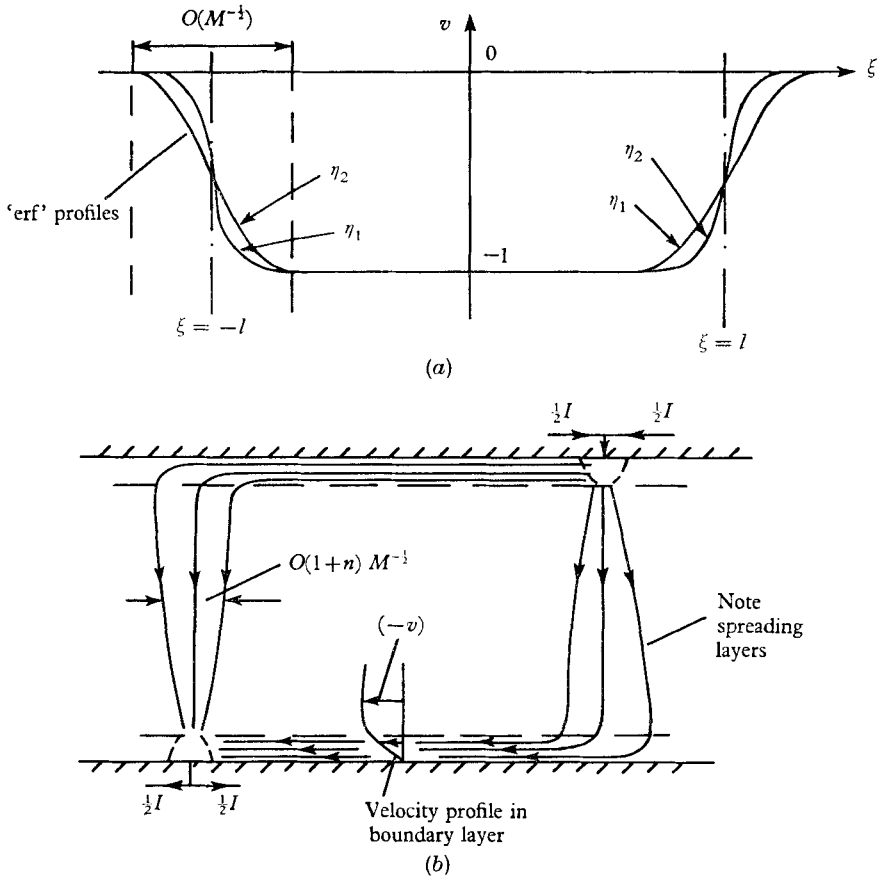

FIGURE 6. Flow between displaced line electrodes when $M \gg 1$. (*a*) Schematic velocity profiles in regions (1) and (4) at constant values of η, $\eta = \eta_1, \eta_2$ where $\eta_2 > \eta_1$. (*b*) Current streamlines, and a velocity profile in region (2).

electrodes were finite, such that there was a finite potential difference $\Delta\phi$ between them, it would be found that the relation between Q and $\Delta\phi$ depends on B_0. This result was to be expected since Hunt & Stewartson (1965), who examined the flow in a rectangular duct with perfectly conducting walls parallel to the field, showed that for such a flow when there is no pressure gradient the first term in the $Q-I$ relation is independent of B_0, whereas the $Q-\Delta\phi$ relation is not. It is also worth noting that the first term in (2.24) is the same as that of the $Q-I$ relation for a rectangular duct with sides $2a$ and $2b$. This is to be expected since the distribution of current density along the lines $x = \pm b$ does not affect the first term in (2.24).

3. Aligned point electrodes

3.1. *Exact solution*

The disadvantage of studying flows due to line electrodes is that such flows are difficult to produce experimentally. Inevitably at the end of the container enclosing the fluid some recirculation occurs which may upset the flow elsewhere.

However, if circular flows are used there are no such end effects, although the flow, being more unstable entails other problems.

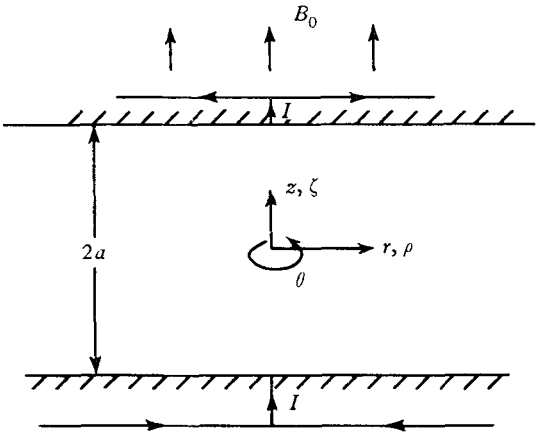

FIGURE 7. Cross-section of the flow induced by aligned point electrodes with a magnetic field, B_0, in the z-direction.

We consider the axisymmetric flow induced by two point electrodes set in insulating planes opposite to each other (see figure 7). Such flows inevitably induce radial pressure gradients which in turn induce radial flow, but if the magnetic field is strong enough, the radial flow is suppressed and the radial pressure gradient may be ignored.† We make the same assumption again only considering the azimuthal or swirl component of velocity, and the radial and axial components of current. Then, in terms of v_θ and H_θ, the azimuthal components of velocity and induced magnetic field, the governing equations are:

$$0 = B_0 \frac{\partial H_\theta}{\partial z} + \tilde{\eta}\left(\frac{\partial^2}{\partial r^2} + \frac{1}{r}\frac{\partial}{\partial r} - \frac{1}{r^2} + \frac{\partial^2}{\partial z^2}\right) v_\theta, \tag{3.1}$$

$$0 = B_0 \frac{\partial v_\theta}{\partial z} + \frac{1}{\sigma}\left(\frac{\partial^2}{\partial r^2} + \frac{1}{r}\frac{\partial}{\partial r} - \frac{1}{r^2} + \frac{\partial^2}{\partial z^2}\right) H_\theta. \tag{3.2}$$

Let the current entering the electrode on the wall at $z = -a$ and leaving the electrode on the wall at $z = +a$, be I, then the boundary conditions are:

$$\text{at } z = +a: \quad rH_\theta = I/2\pi,$$
$$v_\theta = 0;$$
$$\text{at } z = 0: \quad v_\theta \text{ and } H_\theta \text{ are continuous.}$$

We now non-dimensionalize in terms of I:

$$v = \frac{v_\theta}{I/a(\sigma\tilde{\eta})^{\frac{1}{2}}}, \quad h = \frac{H_\theta}{I/(2\pi a)}, \quad \Phi = \frac{\phi}{I/(2\pi a\sigma)} \quad (\rho = r/a,\ \zeta = z/a)$$

and $M = B_0 a(\sigma/\tilde{\eta})^{\frac{1}{2}}$. Then (3.1) and (3.2) become

$$M\frac{\partial h}{\partial \zeta} + \frac{\partial}{\partial \rho}\left(\frac{1}{\rho}\frac{\partial(\rho v)}{\partial \rho}\right) + \frac{\partial^2 v}{\partial \zeta^2} = 0, \tag{3.3}$$

$$M\frac{\partial v}{\partial \zeta} + \frac{\partial}{\partial \rho}\left(\frac{1}{\rho}\frac{\partial(\rho h)}{\partial \rho}\right) + \frac{\partial^2 h}{\partial \zeta^2} = 0. \tag{3.4}$$

† For a more detailed discussion of this point and experimental evidence see Hunt & Malcolm (1968).

We can rewrite these equations as one in $\rho(v+h)$

$$\frac{M}{\rho}\frac{\partial}{\partial\zeta}(\rho(v+h))+\left(\frac{1}{\rho}\frac{\partial^2}{\partial\zeta^2}+\frac{\partial}{\partial\rho}\left(\frac{1}{\rho}\frac{\partial}{\partial\rho}\right)\right)[\rho(v+h)]=0 \tag{3.5}$$

and the boundary conditions become

$$\rho(v+h)=1 \quad \text{at} \quad \zeta=\pm 1. \tag{3.6}$$

The solution of (3.5) subject to the boundary condition (3.6) may be written in terms of Bessel functions:

$$\begin{aligned} v+h=\frac{1}{\rho}&-2\sum_{j=0}^{\infty}\frac{(-1)^j\alpha_j\cosh[\frac{1}{2}M]\,K_1(\lambda_j\rho)\,e^{-\frac{1}{2}M\zeta}\cos\alpha_j\zeta}{\lambda_j}\\ &+2\sum_{j=0}^{\infty}\frac{(-1)^j\beta_j\sinh[\frac{1}{2}M]\,K_1(\mu_j\rho)\,e^{-\frac{1}{2}M\zeta}\sin\beta_j\zeta}{\mu_j}, \end{aligned} \tag{3.7}$$

where $\alpha_j=(j+\frac{1}{2})\pi$, $\beta_j=j\pi$, $\lambda_j^2=\alpha_j^2+M^2/4$, $\mu_j^2=\beta_j^2+M^2/4$ and $K_1(x)$ is a modified Bessel function of the second kind.

3.2. *Asymptotic solution*

As we have found before, the asymptotic solution is simpler and physically clearer. Dividing the flow into three regions as in figure 2 with region (1) lying between the electrodes, regions ($2a$) and ($2b$) lying on the two walls, and regions (3) extending a distance $O(M^{-1})$ round the electrodes, then in regions ($2a$) and ($2b$), (3.5) becomes:

$$\left(\frac{\partial^2}{\partial\zeta^2}+M\frac{\partial}{\partial\zeta}\right)(\rho(v+h))=0, \tag{3.8}$$

and the solution in ($2a$) is $\rho(v+h)=1$.

In region (1), $\partial/\partial\zeta=O(1)$, $\partial/\partial\rho=O(M^{\frac{1}{2}})$ and $\rho=O(M^{-\frac{1}{2}})$ and therefore (3.5) becomes

$$\left\{\frac{1}{\rho}M\frac{\partial}{\partial\zeta}+\frac{\partial}{\partial\rho}\left(\frac{1}{\rho}\frac{\partial}{\partial\rho}\right)\right\}(\rho(v+h))=0. \tag{3.9}$$

The boundary conditions are

$$\rho(v+h)=1 \quad \text{as} \quad \rho\to\infty \quad \text{and when} \quad \zeta=1.$$

Thence

$$\rho(v+h)_1=1-\exp\{-M\rho^2/4(1-\zeta)\}. \tag{3.10}$$

In region ($2b$), the solution to (3.8) is

$$\rho(v+h)_{2b}=1-\exp\{-\{M\rho^2/[4(1-\zeta)]\}\}[1-\exp\{-M(1+\zeta)\}]. \tag{3.11}$$

By considering the symmetry of the flow we see that in (1),

$$v=\frac{1}{2\rho}\{\exp\{-M\rho^2/[4(1+\zeta)]\}-\exp\{-M\rho^2/[4(1-\zeta)]\}\} \tag{3.12}$$

and

$$h=\frac{1}{2\rho}\{2-\exp\{-M\rho^2/[4(1+\zeta)]\}-\exp\{-M\rho^2/[4(1-\zeta)]\}\}. \tag{3.13}$$

Though the form of the velocity profile is similar to that for the line electrode, the important difference is that in this case

$$v = O(M)^{\frac{1}{2}},$$

whereas for a line electrode, $v = O(1)$.

We can also deduce this result by an order of magnitude argument.

In the region (1),

$$\begin{aligned} B_0 v_\theta &\simeq \partial\phi/\partial r \\ &= O[\phi_{r=0}/\delta], \end{aligned}$$

where $\delta = O(M^{-\frac{1}{2}})$ is the thickness of region (1) and, since at $r = 0$,

$$\begin{aligned} \phi &= O(Ia/\sigma\pi\delta^2) \\ &= O(IM/a), \\ v_\theta &= O\left[\frac{IM}{\sigma a}\frac{M^{\frac{1}{2}}}{a}\frac{1}{B_0}\right] \\ &= O\left[\frac{IM^{\frac{1}{2}}}{a(\sigma\eta)^{\frac{1}{2}}}\right]. \end{aligned}$$

For a line electrode, at $x = 0$, $\phi = O[Ia/\sigma\delta]$,

and thence $v_\theta = O[I/\sqrt{\sigma\eta}]$,

where I in this case is the current passing between the electrodes per unit length. Thus the different values of v_θ in terms of M result from the much higher potential which occurs in the point electrode case than the line electrode case.

We also note that if the exact solution is examined as $M \to \infty$, it may be shown to be identical to the asymptotic solution in regions (1) and (2), see appendix C.

J.C.R.H. would like to thank Professor J. A. Shercliff for originally raising his interest in the problem and to the Central Electricity Generating Board for supporting him at the University of Warwick while this work was being done. Finally J.C.R.H. would like to acknowledge that the manuscript of the paper was partly prepared while a visiting lecturer at the Department of Electrical Engineering, University of Cape Town.

Appendix A. Asymptotic form of exact solution for aligned line electrodes

For large M the solution X of §2.1 is given by (2.13),

where

$$X = \frac{2}{\pi}\int_0^\infty \frac{g(\eta,\alpha)\sin\alpha\xi}{\alpha}\,d\alpha,$$

$$\begin{aligned} g \sim \exp\{\tfrac{1}{2}M(1-\eta)\}[\exp\{-(1-\eta)\mu\} - \exp\{-(3+\eta)\mu\}] + \exp\{\tfrac{1}{2}M(1+\eta)\} \\ \times [\exp\{-(1+\eta)\mu\} - \exp\{-(3-\eta)\mu\}], \end{aligned} \quad \text{(A 1)}$$

from (2.14).

Away from regions of $O(M^{-1})$ near the walls $\eta = \pm 1$ the last three terms in (A 1) are negligible compared to the first and hence in region 1

$$X \sim \frac{2}{\pi}\exp\{\tfrac{1}{2}M(1-\eta)\}\int_0^\infty \frac{\sin\alpha\xi}{\alpha}\exp\{-(1-\eta)\mu\}\,d\alpha$$

$$= \frac{\exp\{\tfrac{1}{2}M(1-\eta)\}}{\pi i}\int_{-\infty}^{\infty} \frac{e^{i\alpha\xi}\exp\{-(1-\eta)\mu\}}{\alpha}\,d\alpha. \tag{A 2}$$

Equation (A 2) may be rewritten, on making the change of variable

$$2\alpha = M\sinh(x+i\psi),$$

as
$$X \sim \frac{1}{\pi i}\exp\{\tfrac{1}{2}M(1-\eta)\}\int_{-\infty-i\psi}^{\infty-i\psi} \exp\{-\tfrac{1}{2}Mr\cosh x\}\coth(x+i\psi)\,dx, \tag{A 3}$$

where $r^2 = (1-\eta)^2+\xi^2$ and $\tan\psi = \xi/(1-\eta)$. The contour of integration in (A 3) may now be deformed into the real axis giving

$$X \sim \frac{1}{\pi i}\exp\{\tfrac{1}{2}M(1-\eta)\}\Big\{\int_{-\infty}^{\infty} \exp(-\tfrac{1}{2}Mr\cosh x)\coth(x+i\psi)\,dx \pm H(\pm\psi)\exp\{\tfrac{1}{2}M(1-\eta)\}\Big\}, \tag{A 4}$$

where H is the Heaviside function.

The integration in (A 4) appears at first sight to be of a type which may be evaluated by the method of steepest descent; however, for small ψ the integrand has a pole near the saddle-point and the steepest descent method must be modified. A similar situation occurs in electromagnetic scattering theory in evaluating the field variation across the shadow boundary and the necessary modification to the steepest descent method has been discussed by Clemmow (1950). Application of this modified saddle-point to (A 4) gives

$$X \sim \frac{\cos\psi}{\cos\tfrac{1}{2}\psi}[\operatorname{erfc}\{-(Mr)^{\frac{1}{2}}\sin\tfrac{1}{2}\psi\}-2H(\psi)] \pm H(\pm\psi). \tag{A 5}$$

Equation (A 5) is valid for all ψ; however, in region 1 where $\xi = O(M^{-\frac{1}{2}})$, the cosines may be replaced by unity and $\sin\frac{1}{2}\psi$ by $\xi/2(1-\eta)^{\frac{1}{2}}$ and hence in this region

$$X \sim \operatorname{erf}\frac{M^{\frac{1}{2}}\xi}{2(1-\eta)^{\frac{1}{2}}}, \tag{A 6}$$

in agreement with (2.16).

Form in regions (2*a*)

Inspection of (A 1) shows that in the neighbourhood of $\eta = 1$ the dominant term is still the first and hence (A 6) is still valid in regions 2*a*. In these regions however $\xi M^{\frac{1}{2}}/(1-\eta)^{\frac{1}{2}}$ is $O(M^{\frac{1}{2}})$ and hence the error function may be replaced by $\pm H(\pm\xi)$, in agreement with (2.18).

Form in regions (2*b*)

In the neighbourhood of $\eta = -1$ the first three terms on the right-hand side of (A 1) are equally dominant and hence in regions 2*b*

$$-X \sim \frac{1}{\pi_i}\int_{-\infty}^{\infty} \frac{e^{i\alpha\xi}}{\alpha}\{\exp\{\tfrac{1}{2}M(1-\eta)\}[\exp -\{(1-\eta)\mu\} - \exp\{-(3+\eta)\mu\}] + \exp\{-\tfrac{1}{2}M(1+\eta) - (1+\eta)\mu\}\}\,d\alpha. \quad \text{(A 7)}$$

The terms on the right-hand side of (A 7) are a linear combination of those occurring in (A 2) and it follows by inspection of the analysis leading to (A 6) that (A 7) becomes

$$X \sim \operatorname{erf}\frac{\xi M^{\frac{1}{2}}}{2(1-\eta)^{\frac{1}{2}}} - \exp\{-M(1+\eta)\}\operatorname{erf}\frac{\xi M^{\frac{1}{2}}}{2(\eta+3)^{\frac{1}{2}}} + \exp\{-M(1+\eta)\}\operatorname{erf}\frac{\xi M^{\frac{1}{2}}}{2(\eta+1)^{\frac{1}{2}}}. \quad \text{(A 8)}$$

In the first two terms of (A 8) η may be replaced by -1, also in regions 2*b* $\xi M^{\frac{1}{2}}/(1+\eta)^{\frac{1}{2}}$ is $O(M^{\frac{1}{2}})$ and the error function may thus be replaced by $\pm H(\pm\xi)$ thus giving

$$X \sim \pm H(\pm\xi)\exp\{-M(1+\eta)\} + [1-\exp\{-M(1+\eta)\}]\operatorname{erf}\frac{\xi M^{\frac{1}{2}}}{8^{\frac{1}{2}}}, \quad \text{(A 9)}$$

which agrees with (2.19).

Appendix B. Fourier integral for displaced line electrodes

For the case of the displaced line electrodes of §2.3 the exact solution for X is given by

$$X = \frac{2}{\pi}\left\{\exp\{\tfrac{1}{2}M(1-\eta)\}\int_0^\infty \frac{\sinh\mu(1+\eta)}{\alpha\sinh 2\mu}\sin\alpha(\xi-l)\,d\alpha - \exp\{\tfrac{1}{2}M(1+\eta)\}\int_0^\infty \frac{\sinh\mu(1-\eta)}{\alpha\sinh 2\mu}\sin\alpha(\xi+l)\,d\alpha\right\}.$$

The appropriate asymptotic forms for this case may be derived by an obvious extension of the arguments leading to equations (A 6) and (A 9) and are in agreement with the results obtained in §2.3.

Appendix C. Asymptotic form of the solution for point electrodes

Replacing the hyperbolic functions in (3.7) by $\frac{1}{2}\exp(\frac{1}{2}M)$ and making use of the identity (Erdelyi, Magnus & Oberfettinger 1954)

$$\frac{K_1[a(b^2+c^2)^{\frac{1}{2}}]}{(b^2+c^2)^{\frac{1}{2}}} = \frac{1}{ab}\int_a^\infty \sin b(t^2-a^2)^{\frac{1}{2}}\,e^{-ct}\,dt$$

shows that, for large M,

$$v+H \sim \frac{1}{\rho} - \frac{2}{M}\exp\{\tfrac{1}{2}M(1-\zeta)\}\int_\rho^\infty \sin\tfrac{1}{2}M(t^2-\rho^2)^{\frac{1}{2}}\left[\sum_{j=0}^{\infty}(-)^j e^{-\alpha_j t}a_j\cos\alpha_j\zeta + \sum_{j=1}^{\infty}(-)^j e^{-\beta_j t}\beta_j\sin\beta_j\zeta\right]dt. \quad \text{(C 1)}$$

The summation in (C 1) may be carried out giving

$$v+H \sim \frac{1}{\rho}+\frac{2}{M}\exp\{\tfrac{1}{2}M(1-\zeta)\}\int_{\rho}^{\infty}\sin\tfrac{1}{2}M(t^2-\rho^2)^{\frac{1}{2}}\frac{df}{dt}dt,$$

where

$$f(t)=\frac{\cos\frac{1}{2}\pi\zeta}{[\cosh\frac{1}{2}\pi t-\sin\frac{1}{2}\pi\xi]}.$$

Integration by parts and some slight manipulation then gives

$$v+H \sim \frac{1}{\rho}-\frac{\exp\{\frac{1}{2}M(1-\zeta)\}}{2}\int_{-\infty}^{\infty}\exp\{\tfrac{1}{2}iM\omega\}f[(\omega^2+\rho^2)^{\frac{1}{2}}]\,d\omega. \qquad \text{(C 2)}$$

The contour may now be completed by a large semi-circle in the upper half plane and the right-hand side of (B 2) may then be replaced by a residue series. The integrand has poles at $\omega^2=-\rho^2-[2(2n+1)\pm(1+\zeta)]^2$, n integer, these give rise to exponentially damped terms in the residue series and the dominant contributions arise when $n=0$. After some elementary manipulation it follows that

$$\rho(v+H) \sim 1-\exp\{\tfrac{1}{2}M(1-\zeta)\}\frac{(1-\zeta)}{[\rho^2+(1-\zeta)^2]^{\frac{1}{2}}}\exp\{-\tfrac{1}{2}M[\rho^2+(1-\zeta)^2]^{\frac{1}{2}}\}$$

$$+\exp\{\tfrac{1}{2}M(1-\zeta)\}\frac{[3+\zeta]}{\{\rho^2+(3+\zeta)^2\}^{\frac{1}{2}}}\exp\{\tfrac{1}{2}M[\rho^2+(3+\zeta)^2]^{\frac{1}{2}}\}.$$

Equation (C 3) is exact in the sense that the terms neglected are everywhere exponentially damped compared to those retained and the equation is valid everywhere. It is easily verified that (C 3) reduces in the appropriate regions to yield the results of §3.2.

REFERENCES

Alty, C. J. N. 1966 Ph.D. Thesis, Cambridge University.

Braginskii, S. I. 1960 *Sov. Phys.* (*JETP*) **10**, 1005.

Childress, S. 1963 *J. Fluid Mech.* **15**, 429.

Clemmow, P. C. 1950 *Q. J. Mech. Appl. Math.* **3**, 241.

Erdelyi, A., Magnus, W. & Oberfettinger, F. 1954 *Table of Integral Transforms*, **1**, 154.

Hasimoto, H. 1960 *J. Fluid Mech.* **8**, 61.

Hunt, J. C. R. 1968 To appear in *Proc. Camb. Phil. Soc.*

Hunt, J. C. R. & Malcolm, D. G. 1968 To appear in *J. Fluid Mech.*

Hunt, J. C. R. & Stewartson, K. 1965 *J. Fluid Mech.* **23**, 563.

Ludford, G. S. S. 1961 *J. Fluid Mech.* **10**, 141.

Moffatt, H. K. 1964 *Proc. 11th Int. Cong. Appl. Mech., Munich*, pp. 946–953.

Shercliff, J. A. 1953 *Proc. Camb. Phil. Soc.* **49**, 136.

Shercliff, J. A. 1965 *A Textbook of Magnetohydrodynamics.* Oxford: Pergamon Press.

Waechter, R. T. 1966 Ph.D. Thesis, Cambridge University.

Yakubenko, A. Ye 1963 *Zh. Prikl. Mech. Teck. Fiz.* no. 6, 1963. *NASA Transl.* F-241, Sept. 1964.